Bull. Mater. Sci., Vol. 38, No. 3, June 2015, pp. 593–598. © Indian Academy of Sciences.

Thermally assisted variable range hopping in Tl_4S_3Se crystal

ABDELHALIM M ZIQAN[1], A F QASRAWI[1,2,*], ABDULFTAH H MOHAMMAD[1] and N M GASANLY[3]

[1]Departments of Mathematics and Physics, Arab American University, Jenin 240, Palestine
[2]Group of Physics, Faculty of Engineering, Atilim University, 06836 Ankara, Turkey
[3]Department of Physics, Middle East Technical University, 06800 Ankara, Turkey

MS received 18 April 2014; revised 13 August 2014

Abstract. **In this study, a modified model for the application of the thermionic and hopping current conduction mechanisms in the presence of continuous mixed conduction is investigated, discussed, experimented and simulated. It is observed that there exists a contribution from the hopping conductivity to the total conduction even at temperature ranges where the thermionic emission is mainly dominant. The contribution weight of a specific mechanism at particular temperature range is estimated. In addition, a modification to the Mott's variable range hopping (VRH) transport parameters like density of localized state near the Fermi level, the average hopping range and the hopping energy in the presence of mixed conduction mechanism is also reported. This new approach corrects the evaluated electrical parameters that are necessary for the construction of electronic devices like absorption layers in solar cells. This proposed model is also used to explain the conduction mechanism and investigate the electrical conduction thermionic and Mott's VRH parameters in Tl_4S_3Se crystals and in $CuAlO_2$ thin films.**

Keywords. **Variable range hopping; mixed conduction; thermionic; Tl_4S_3Se crystal.**

1. Introduction

Owing to the vital role of the electronic transport on the performance of electronic devices, the conduction mechanism of charge carriers in solid materials has been attracting the interest of researchers since decades. Chen *et al*[1] have studied the hopping conduction effect on the $Zn:SiO_2$ resistive random-access memory (RRAM) device. Their analysis has shown that the accumulation of metallic ions lead to the shortening of the hopping range, which in turn lowers the activation energy of the charge carrier. In addition, the tunnelling current conduction in a resistive switching memory, fabricated with anodic aluminium oxide, was found to decrease the reproducibility of switching voltages.[2] The conduction and switching mechanisms of $Al/AlO_x/WO_x/W$ bilayer RRAM devices were also found to vary with electrical resistance states. Particularly, at low resistance levels, the RRAM devices exhibited Ohmic conduction with metallic behaviour. For moderate resistance levels, the current transport is reported to be dominated by electron hopping; when the resistance level is high the conduction was governed by Schottky emission.[3]

Recent studies[4–7] focused on the mixed conduction between more than one types of conduction mechanism. As for example, the thermionic emission of charged particles over an energy barrier is found to be associated with the assistance of variable range hopping (VRH) in $TlInSe_2$ crystals.[4] Most of the published works that consider the mixed conduction between two transport mechanisms assume the validity of one mechanism at a particular temperature range and the validity of the other at another range. The mixing is just in an intermediate short range of temperature. In other cases, it happens that one type of conduction dominates but with different activation energy values. For this case, there must be a particular electronic contribution in the conduction from a shallow activation level to a deeper one that dominates at higher temperatures. Thus, here in this work we follow a simple mathematical approach that analyses, simulates and explains the contribution between more than one transport mechanisms. The study will provide information about the role of the electronic activation of the non-dominant conduction mechanism to the dominant ones. This modified approach to the total conduction mechanism will be applied to explain the electrical conduction mechanism in Tl_4S_3Se single crystal, which will be reported for the first time. It will also be used to explain the reasons beyond the difference in the values of the published electrical parameters data of $CuAlO_2$ thin films.

2. Experimental and simulation details

Tl_4S_3Se single crystals were prepared by the Bridgman method from the stoichiometric melts of the starting materials sealed in evacuated (10^{-5} Torr) silica tubes with a tip at the bottom. The sample structure was determined by Philips PW1740 X-ray diffractometer equipped with CuKα

*Author for correspondence (aqasrawi@atilim.edu.tr, aqasrawi@aauj.edu)

radiation ($\lambda = 0.154049$ nm). The crystal is found to exhibit a body centred tetragonal type structure. The lattice parameters are found to be $a = 0.7827$ and $c = 0.6795$ nm. The contacts to the samples were done by using a silver paste (Agar Scientific-Electrodag 1415 M). The electrical conductivity was recorded by means of Lake Shore 7507 Hall-effect measurement system. The data were collected using an IEEE computer interface and IDEAS software provided by Lake Shore.

The simulation was handled with the help of MATlab software. The software was used to design computer programs capable of carrying out multi-operations on current conduction mechanism. The designed software link loops to provide a temperature-dependent conductivity display and obtains the best fitting parameters for each applied mathematical equation.

3. Review of existing models

Band conduction in solid materials is mainly dominated by the thermal excitation of charge carriers. It exhibits an activation type of conduction, in which the electrical conductivity (σ_{Th}) is mathematically defined by the function

$$\sigma_{\mathrm{Th}} = \sigma_0 \exp\left(-E_\sigma / kT\right) \tag{1}$$

with $E_\sigma = E_\mathrm{c} - E_\mathrm{F}$ or $E_\sigma = E_\mathrm{F} - E_\mathrm{v}$ being the electron activation energy in n-type semiconductor or hole activation energy in p-type semiconductor, respectively.[8] Here E_F, E_c and E_v are the Fermi energy, the conduction band energy and the valence band energy levels, respectively. Due to the temperature dependence of the energy bandgap $\left(E_\mathrm{g} = E_\mathrm{c} - E_\mathrm{v}\right)$, the value of $E_\mathrm{c} - E_\mathrm{F}$ is also regarded as temperature dependent. For linear variation of the energy bandgap with temperature, the E_σ value is reedited to take the form $E_{\sigma 0} - \delta T$, where δ is the rate of change of E_σ with temperature and is given in (eV/K). In this case the conductivity function can be rewritten as

$$\sigma_{\mathrm{Th}} = \sigma_0^1 \exp\left(-E_{\sigma 0} / kT\right) \tag{2}$$

with

$$\sigma_0^1 = \sigma_0 \exp\left(\delta / k\right). \tag{3}$$

Another reason for the variation of $E_\sigma(T)$ with temperature arises from the statistical shift of E_F, which is brought about the energy dependence of the density of state spectrum. For this case $E_{\sigma 0}$ becomes temperature dependent. When this effect is considered in the pre-exponential factor, σ_0^1 of eq. (2), E_σ of eq. (1) becomes temperature independent quantity. Meyer–Neldel rule (MNR)[8,9] assumes a temperature dependence between σ_0 and E_σ in accordance to the relation,

$$\sigma = \sigma_0^2 \exp\left(AE_\sigma / kT\right), \tag{4}$$

where A is constant and σ_0^2 is the new pre-exponential factor. Abtew *et al*[9] have shown that for the validity of MNR, the existence of the localized states and the energy dependence of the electron-lattice coupling are essential conditions. The decrease in $E_\sigma(T)$ with decreasing T appears as a result of the multi-excitation through the localized states whose transition has an activation energy decreasing with temperature. The transition through these localized states includes the hopping transport of charge carriers over the energy barriers. The details of this theory are clearly discussed in the study by Abtew *et al*.[9] In the current study, it is sufficient to recall that the variation of $E_\sigma(T)$ with temperature depends on the value of A (see eq. (4)). The A value includes all the information about the linear variation of $E_\sigma(T)$ with T.

Based on the above-mentioned ideas, we remind that there exist temperature regions in which finding linear slopes for the $\ln(\sigma(T)) - T^{-1}$ variation was not possible.[4,9] For these cases, the continuously changing $E_\sigma(T)$ was ascribed to the existence of VRH. The hopping conduction occurs through unoccupied localized levels near the Fermi level. When the localized levels are distributed quasi continuously, the hopping between two sites, whose energy difference, W, is small, becomes most probable. The hopping probability increases with a factor of $\exp(-W / kT)$. Thus, charged particles hop to the most probable site. The hopping conductivity $\sigma_{\mathrm{hp}}(T)$ is given by Morigaki,[8] Abtew *et al*,[9] Qasrawi,[10] Mott and Davis,[11]

$$\sigma_{\mathrm{hp}}(T) = \sigma_2 \exp\left(-\left(\frac{T_0}{T}\right)^{1/4}\right), \tag{5}$$

where

$$\sigma_2 = e^2 a^2 \nu_{\mathrm{ph}} N(E_\mathrm{F}) \tag{6}$$

and the degree of disorder,

$$T_0 = \frac{\lambda \gamma^3}{k_\mathrm{B} N(E_\mathrm{F})}. \tag{7}$$

Here, a is the hopping distance, $\nu_{\mathrm{ph}} \sim 10^{13}$ s^{-1} is the phonon frequency, $N(E_\mathrm{F})$ is the density of localized states near the Fermi level and γ—the inverse of localization length (ξ)—is the decay constant. λ is a dimensionless constant based on percolation parameter and is equal to 18–49.[10] The average hopping distance, R, and the average hopping energy, W, are usually evaluated with the help of the following equations:[8,11]

$$R = \left(\frac{9}{8\pi\gamma k_\mathrm{B} T N(E_\mathrm{F})}\right)^{1/4} \tag{8}$$

and

$$W = \frac{3}{4\pi R^3 N(E_\mathrm{F})}. \tag{9}$$

4. Statement and solution to the mixed conduction problem

The variation of the activation energy with temperature can be easily recognized by reediting eq. (1) as, $E_\sigma(T)/kT =$

$\ln(\sigma\ (T) - \ln(\sigma_0)$ and executing the first derivative of $E_\sigma\ (T)$ numerically through the equation,

$$\mathrm{d}E_\sigma\ (T) = -\frac{\mathrm{d}\left(\ln(\sigma) - \ln(\sigma_0)\right)}{\mathrm{d}\left(kT^{-1}\right)}. \tag{10}$$

If the pre-exponential factor σ_0 is temperature independent, the obtained $\mathrm{d}E_\sigma(T)$ from the numerical derivation of natural algorithm of the conductivity with respect to $(kT)^{-1}$ must exhibit constant incremental values in particular temperature ranges. Such behaviour is clearly shown in the figures of $\mathrm{d}E_\sigma - T$, which was previously given.[4,10,12] However, as the statistical Fermi level shifts with temperature, the value of E_σ changes over wide temperature ranges. Further, as E_σ could exist due to the impurities, broken bonds and material inhomogeneities, it may reserve particular location in the energy bandgap. The excitation of these levels depends on the thermal energy. Thus, E_σ will always change depending on the minimum thermal energy needed for excitation. As temperature decreases, the kT energy value becomes less effective in conducting electrons located at deep level from the minimum of the conduction band. Thus, there are regions in which more than one E_σ shares in the conduction.

As another look to the mixed conduction problem, we will assume that the conductivity is governed by a set temperature independent conductivity activation energies $E_{\sigma1}$, $E_{\sigma2}$ and $E_{\sigma3}$, being dominant in particular temperature ranges $\Re_1$, $\Re_2$ and $\Re_3$, respectively. The temperature range $\Re_1$ is higher than $\Re_2$, and $\Re_2$ is higher than $\Re_3$. There are three cases to be considered:

(i) The electrical conduction is governed by the thermionic emission of charge carriers from $E_{\sigma1}$, $E_{\sigma2}$ and $E_{\sigma3}$ with one of them dominant over the others. The value of kT determines which energy level is most dominant. The traditional method of determining these activation energy levels is by assuming the validity of eq. (1) in each temperature range and plotting $\ln\sigma\ (T) - T^{-1}$. The slope and intercept of this plot allows to determine E_σ and σ_0, respectively. This way of evaluation assumes no contribution from one activation level to another. The total conductivity ($\sigma = \sigma_1 + \sigma_2 + \sigma_3 + \cdots$) of a material that has more than one activation energy level E_σ is then defined by series,

$$\begin{aligned}\sigma\ (T) &= \sum_{j=1}^{n} \sigma_{0j} \exp(-E_{\sigma j} / kT) \\ &= \sigma_{01} e^{-E_{\sigma1}/kT} + \sigma_{02} e^{-E_{\sigma2}/kT} + \sigma_{03} e^{-E_{\sigma3}/kT} + \cdots\end{aligned} \tag{11}$$

Here, as previously mentioned, $E_{\sigma1}$, $E_{\sigma2}$ and $E_{\sigma3}$ are dominant in particular temperature ranges $\Re_1$, $\Re_2$ and $\Re_3$, respectively. When this tradition procedure is applied to evaluate the conductivity activation energy of Tl_4S_3Se single crystals (for example), which are displayed as open circles in figure 1, $E_{\sigma1}$, $E_{\sigma2}$ and $E_{\sigma3}$ are found to be 178, 93 and 47 meV, in $\Re_1 = 300$–250 K, $\Re_2 = 230$–150 K and $\Re_3 = 120$–50 K ranges, respectively. The corresponding σ_{01}, σ_{02} and σ_{03} values are 7.08×10^{-2}, 4.34×10^{-4} and $1.29 \times 10^{-5}(\Omega\ \mathrm{cm})^{-1}$.

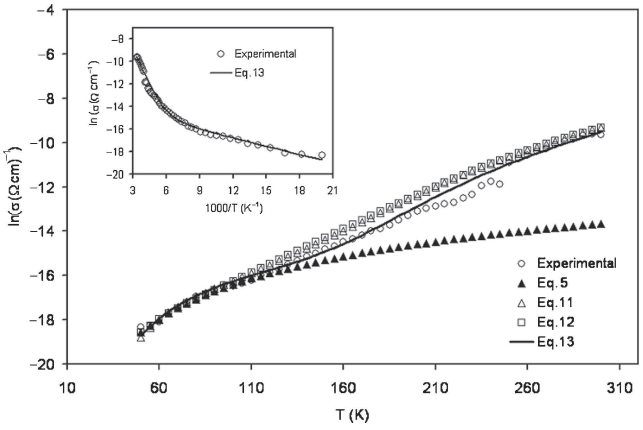

Figure 1. The temperature dependence of the electrical conductivity for Tl_4S_3Se crystal. The inset shows the reciprocal dependence.

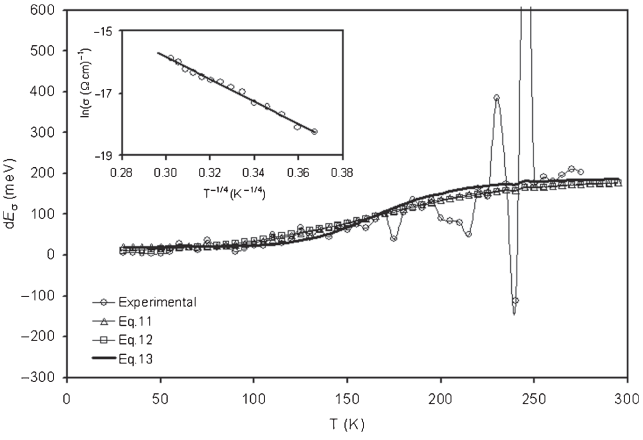

Figure 2. The $\mathrm{d}E_\sigma - T$ dependence for Tl_4S_3Se crystal. The inset shows the hopping conductivity in accordance to eq. (5).

To get information about the correlation between the obtained results assuming the validity of eq. (1), a simulator was designed with the help of MATlab software. The simulator allows the entry of $E_{\sigma j}$ and σ_{0j}values. The results of the simulator, using eq. (11), are displayed (marked by triangles) in figure 1. Consistently, $\mathrm{d}E_\sigma$ for the experimental conductivity and the conductivity evaluated assuming the validity of eq. (11) by the simulator is displayed in figure 2. Even though the $\mathrm{d}E_\sigma - T$ variance revealed some poor consistency between the experimental and the one evaluated using eq. (11), figure 1 reflects good agreement between the experimental and simulated data in $\Re_1 = 300$–250 K range only. The simulated conductivity data did not agree with the experimental one in $\Re_2$ and $\Re_3$ ranges.

The inconsistency between the experimental and simulated data indicates that the assumption that the $E_{\sigma j}$ values are independent of each other and no contribution from one $E_{\sigma j}$ to another are not correct. In addition, in contrast to the behaviour of the simulated $\mathrm{d}E_\sigma$, for all T values that lie in $\Re_2$ and $\Re_3$ ranges, $\mathrm{d}E_\sigma$ continuously decreases with decrease

in T. This behaviour is clearly different from that we have previously reported.[4,10] For these reasons a more appropriate approach is described below.

(ii) Now we will assume that, the hopping conduction dominates in $\Re_3 = 120{-}50$ K range and the thermionic emission dominates only in $\Re_1$ and $\Re_2$ ranges. This is the usual method of determining the current transport mechanism in materials. As the thermionic emission is dominant at higher kT and hopping conduction is dominant at lower kT values, there should be no contribution from σ_{hp} to σ_{Th}. Thus, if the condition for the validity of conduction by hopping presented by $T_0 > 10^3$, $N(E_F)$, R, W, $\gamma R \gg 1$ is satisfied, then the hopping transport mechanism dominates and the evaluation of the Mott's VRH parameters becomes straightforward. Following the method described by eqs (5–9) and plotting of $\ln(\sigma) - T^{-1/4}$ (shown in the inset of figure 2), it is possible to determine the value of T_0. Using the slope of the solid line displayed in the inset of figure 2, the Mott's VRH parameters for Tl_4S_3Se crystals are determined and displayed in table 1. The parameters are evaluated for a localization length of 5 Å. The calculated values of the hopping parameters assuming the validity of eq. (5), which is also simulated and presented by solid triangle markers in figure 1, are consistent with literature data and assure the validity of the hopping transport in the low temperature region.

In the scope of the hopping conduction analysis, the total conductivity equation, displayed in eq. (11), becomes

$$\sigma\,(T) = \sigma_{01}e^{-E_{\sigma1}/kT} + \sigma_{02}e^{-E_{\sigma2}/kT} + \sigma_2 e^{-(T_0/T)^{1/4}}. \quad (12)$$

Now by substituting the values of σ_{01}, σ_{02}, σ_2 and T_0 into eq. (12), the total conductivity is re-calculated and plotted in figure 1 as open square markers. The simulated conductivity using eq. (12) is able to reproduce the experimental data at low temperatures only. The evaluated dE_σ from eq. (12) data coincide with the experimental at low temperatures only. This indicates that the assumption of no hopping contribution to the thermionic emission is not appropriate for this problem. As a result we have tried the third possibility of conduction, which can be described as below.

(iii) Overall in kT of electron, the total conductivity is governed by both σ_{Th} and σ_{hp} at the same temperature. In this case, the conductivity is governed by the equation,

$$\sigma = \sigma_{01}e^{-E_{\sigma1}/kT} + \sigma_{02}e^{-E_{\sigma2}/kT} + \sigma_{03}e^{-E_{\sigma3}/kT} + \sigma_2 e^{-(T_0/T)^{1/4}}. \quad (13)$$

The equation indicates that both of the thermionic and hopping conductions are shared at all temperatures. Here, the most important fitting parameter is T_0, because all the other parametersdid not reveal the exact solution. As T_0 indicates the role of the hopping conduction, the simulator is designed in such a way that it allows the entry of $E_{\sigma j}$, σ_{0j} and σ_2, and it finds the right T_0, that reproduce the exact experimental data. For the Tl_4S_3Se crystal T_0 was determined as 3.1×10^6 K. The results of the simulator using eq. (13) are shown by solid line in figures 1 and 2. The consistency between the conductivity evaluated using eq. (13) and the experimental one is also presented as function of reciprocal temperature in the inset of figure 1. The re-evaluated Mott's VRH parameters are also displayed in table 1. As the table shows there is a clear difference between the tabulated data when the hopping conduction is assumed to be dominant in the studied temperature range. Similarly, the probable dE_σ that mostly fits with experimentally evaluated one is the one which is obtained from eq. (13).

It is worth notifying that, the simulation results using eq. (13) did not reveal any of the activation energies obtained by the procedure described in case (i). The activation energy values that best fitted the results are found to be 195, 105 and 21 meV, respectively. The main difference between eqs (12) and (13) is the assumption that the hopping and the thermionic are shared at each temperature and eq. (13) includes an extra activation level ($E_{\sigma3}$) that conducts by thermionic emission.

In an attempt to clarify the proposed idea, which states that the mixed conduction composed of thermionic and VRH is the most probable conduction mechanism at all temperatures in materials exhibiting a set of localized states in its energy bandgap, we have calculated the weight of the contribution of each of the dominant conductivities. The contribution ($\mu = \frac{\sigma_j}{\sigma_T} \times 100\%$) from one activation level to the total conductivity assuming the validity of eq. (13) is displayed in figure 3a. As the figure illustrates, the conduction due to the $E_{\sigma1}$ =195 meV, which in accordance to eq. (1), is found to be 178 meV and is believed to terminate at 250 K and dominates strongly ($\mu > 50\%$) down to 190 K but terminates at ~130 K. On the other hand the 93 meV activation energy, which was dominant in $\Re_2$ range is found to be 105 meV by the simulator, weakly dominates at all temperatures and terminates at ~90 K. Similarly, the 47 meV activation energy reduces to 21 meV. The latter energy level dominates below

Table 1. The evaluated electrical parameter for Tl_4S_3Se crystals and $CuAlO_2$ thin films.

Eq.	E_{01} (meV)	E_{02} (meV)	E_{03} (meV)	γ (cm^{-1}) $\times10^7$	T_0 (K) $\times 10^6$	$N(E_F)$ (cm^3/eV)	R(100 K) (cm) $\times10^{-7}$	W(meV)	γR
					Tl_4S_3Se crystal				
1, 5	178	93	47	2.00	1.70	9.88×10^{20}	2.05	28.2	4.1
12	195	105	0	2.00	1.60	10.49×10^{20}	2.11	24.3	4.2
13	195	105	21	2.00	3.10	5.42×10^{20}	2.38	32.8	4.8
					$CuAlO_2$ thin film				
1, 5	285	0	0	2.00	434.78	3.85×10^{18}	8.57	98.6	17.1
13	285	245	115	2.00	520	3.23×10^{18}	8.96	103.0	17.9

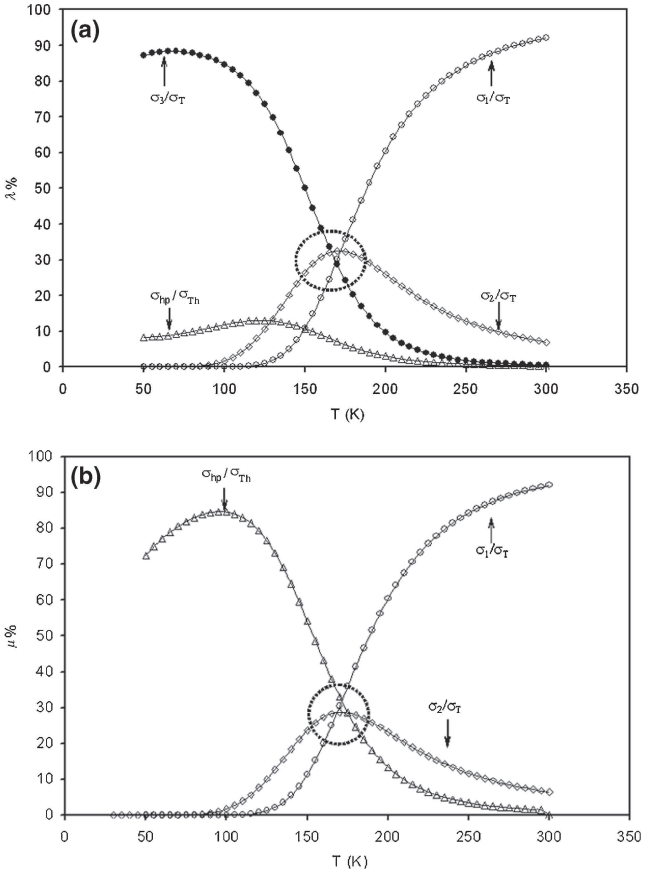

Figure 3. The weight of the conduction contribution for Tl_4S_3Se crystal as estimated assuming the validity of (**a**) eq. (13) and (**b**) eq. (12).

250 K and becomes strongly effective at low temperatures. The hopping conduction contribution to the total conductivity of the Tl_4S_3Se crystal is weakly dominant at all temperatures with a relatively stronger ($\mu \sim 9\%$) effect below 140 K. On the other hand, if $E_{\sigma 3}$ in eq. (13) is assumed to be zero, this equation becomes the same as eq. (12). For this case the simulator reproduces the experimental data with $E_{\sigma 1} = 195$ meV, $E_{\sigma 2} = 105$ meV and $T_0 = 1.6 \times 10^6$ K as fitting parameters. The latter case which is displayed in figure 3b indicates that the hopping conduction dominates even at 300 K with continuously increasing effect and becomes strongest ($\mu \sim 85\%$) at 90 K. The region, where all the conductivities are equally shared, is shown by dashed circles in figure 3a and b.

Since the studied crystals were not intentionally doped, the existence of these activation energy levels in the crystal are thought to originate from the anion vacancies caused by non-stoichiometric chemical reactions and/or stacking faults that take place during the crystal growth. The possibility of the creation of the stacking faults in the chain Tl_4S_3Se crystal is mainly assigned to the weakness of the van der Waals forces between the chains.

Kosyak *et al*[13] have also modelled a mixed conduction equation to reproduce the conductivity data of polycrystalline Cu_2ZnSnS_4 thin films. Kosyak *et al* fitted the temperature-dependent conductivity data with a model that includes Mott variable-range hopping, nearest-neighbour hopping and thermionic emission over grain boundary barriers. This type of modelling provided more detailed information about the electronic structure of Cu_2ZnSnS_4 thin films. Kosyak *et al* model is highly comparable to the approach we have used to investigate the mixed conduction problem.

We have used our proposed model which is presented by eq. (9) to explain the disagreement in the experimental data reported for $CuAlO_2$ crystals.[14] The $CuAlO_2$ films were deposited on c-planes sapphire by radio-frequency reactive sputtering. These films gain the importance and interest due to their transparency and conducting properties. Such features are important for optoelectronic device fabrication. Su *et al* have measured the electrical conductivity as a function of temperature in the temperature range of 95–300 K. Their data were displayed in figure 4 of the published reference by Su *et al*.[14] The figure represents the plot of $\ln(\sigma) - 1000/T$ and the $\ln(\sigma) - T^{-1/4}$ variations for the phase-pure $CuAlO_2$ films. The authors reported the domination of the thermionic emission with activation energy of 285 meV at high temperature. They also reported that the VRH, which dominates at low temperature, exhibits a linear slope of the $\ln(\sigma) - T^{-1/4}$ variation of $144.5^{1/4}$. The latter value corresponds to a T_0 of 4.35×10^8 K. The 285 meV activation energy is reported to be different from those reported by another group, who reported this value as 250 meV at high temperature and hopping at low temperatures.[15] There is no information about the values of Mott's VRH parameters in both articles by Su *et al*[14] and Banerjee *et al*.[15] The reproduced data of $CuAlO_2$ published by Su *et al*[14] is displayed in figure 4a. The first solution trail was performed by following the author's procedure, in which eqs (1) and (5) of this article were applied. These equations were able to reproduce the data above 235 K and below 150 K, respectively. The resulting data of these two equations are displayed in table 1. When eq. (9) of this article is selected and the designed simulator is run, all the experimental data were fitted with activation energies of $E_{\sigma 1} = 285$, $E_{\sigma 2} = 250$, $E_{\sigma 3} = 115$ meV and $T_0 = 5.2 \times 10^8$ K. The consistency

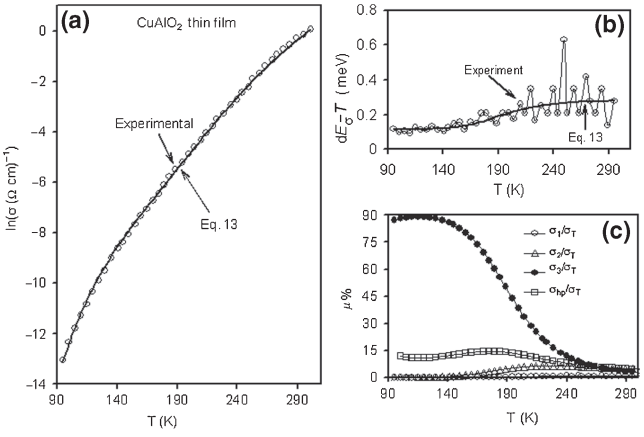

Figure 4. (**a**) The temperature-dependent electrical conductivity, (**b**) The $dE_\sigma - T$ dependence and (**c**) the weight of the conduction contribution for $CuAlO_2$ thin film.

between the experimental data and that of eq. (9) is shown in figure 4a and b for the $\ln(\sigma) - T$ and the $dE_\sigma - T$ (evaluated for the first time here in this article), respectively. To understand the contribution of each type of conductivity to the total conductivity of $CuAlO_2$ films, the $\mu\%$ values were evaluated and are presented in figure 4c. As the figure illustrates, the contribution of the conductivity from the 285 meV level is less than 1%, which means that there is no effective role of this deep energy level in the conduction. On the other hand, the maximum contributions from the 250 meV and from the 115 meV energy levels are ∼7 and 88%, respectively. The hopping conduction never exceeds 15% of the total conduction. Figure 4c suggests that the conduction in $CuAlO_2$ films is of mixed conduction type with the main activation energy level of 115 meV. The conduction due to this level becomes more pronounced with decreasing temperature and reaches its maximum effect at 120 K. This thermionic type activation is mainly shared by the hopping conduction at all temperatures. The tabulated data indicate that the hopping energy for these films are very high compared to those usually observed in thin films. However, because its role in the conduction is less than 15%, assigning the VRH conduction as the main mechanism may lead to ambiguous conclusions.

5. Conclusions

In this study the current transport mechanism theories are reviewed, analysed, simulated and modified. It is concluded that a modified version of conduction must be used to investigate the current transport phenomena in solids. The model is based on the idea that the conduction is governed by mixed conduction that includes current transport by thermionic emission and hopping conduction in the same temperature region. Evaluation of the conductivity equation, which governs all types of conduction, revealed more accurate values of thermal activation energies and Mott's VRH parameters.

References

1. Chen K, Zhang R, Chang T, Tsai T, Chang K, Lou J C, Young T, Chen J, Shih Ch, Tung Ch, Syu Y and Sze S M 2012 *Appl. Phys. Lett.* **102** 133503
2. Otsuka S, Shimizu T, Shingubara S, Iwata N, Watanabe T, Takano Y and Takase K 2013 *ECS Trans*. **50** 49
3. Huaqiang Z Y W, Yue B, An Ch, Zhiping Y, Jinyu Zh and He Q 2013 *Appl. Phys. Lett*. **102** 233502
4. Qasrawi A F and Gasanly N M 2013 *Mater. Chem. Phys.* **141** 63
5. Iwamoto M, Kwon Y S and Lee T 2011 *Nanoscale interface for organic electronics* (Danvers: Word Scientific Publishing Co.)
6. Bellido E P, Bobadilla A D, Rangel N L, Zhong H, Norton M L, Sinitskii A and Seminario J M 2009 *Nanotechnology* **20** 175102
7. Sarker B K and Khondaker S I 2012 *ACS Nano* **6** 4993
8. Morigaki K 1999 *Physics of amorphous semiconductors* (London: Imperial College Press)
9. Abtew T A, Zhang M, Pan Y and Drabold Y A 2008 *J. Non-Cryst. Sol.* **354** 2909
10. Qasrawi A F 2010 *Phil. Mag.* **90** 3027
11. Mott N F and Davis E A 1979 *Electronic process in non crystalline materials* (Clarenton: Oxford)
12. Rubinger R M, Ribeiro G M, de Oliveira A G, Albuquerque H A, Silva R L De, Rubinger C P L, Rodrigues W N and Moreira M V B 2006 *Semicond. Sci. Technol*. **21** 1681
13. Kosyak V, Karmarkar M A and Scarpulla M A 2012 *Appl. Phys. Lett.* **100** 263903
14. Su C T, Lee H Y, Wu B K and Chern M Y 2011 *J. Cryst. Growth* **328** 25
15. Banerjee A N, Maity R and Chattopadhyay K K 2004 *Mater. Lett.* **58** 10